LBL--26651

DE89 012979

Cryogenic Tensile Properties of AA 2090 Weldments

A. J. Sunwoo and J. W. Morris, Jr.

Department of Materials Science and Mineral Engineering
University of California, Berkeley

and

Center for Advanced Materials
Materials and Chemical Sciences Division
Lawrence Berkeley Laboratory
1 Cyclotron Road
Berkeley, California 94720

March 1989

This work is jointly supported by the Director, Office of Energy Research, Office of Basic Energy Science, Materials Sciences Division of the U. S. Department of Energy under Contract No. DE-AC03-76SF00098.

Cryogenic Tensile Properties of AA 2090 Weldments

A. J. Sunwoo and J. W. Morris, Jr.

Center for Advanced Materials, Lawrence Berkeley Laboratory and
Department of Materials Science and Mineral Engineering,
University of California at Berkeley

The influence of base metal temper and filler metal additions on the cryogenic properties of Al-Li 2090 weldments are studied. The results show that as the strength of the base metal increases, strength mismatch increases and the joint efficiency decreases. Inhomogeneous deformation is confined to the fusion zone and the strain localization results in premature failure in the weldment. As the temperature decreases, T3 base metal weldments show better properties than T8 base metal weldments. The influence of filler metal additions on the weldment properties shows that the strengths is limited without post-weld aging, but the increase in elongation is significant. At 77 K, a 6 Cu addition to 2090 yields the best UTS and elongation combination of the filler metals studied. Mg addition leads to embrittlement at 77 K.

Introduction

The 2090-T8E41 Al-Li alloy has very good mechanical properties at cryogenic temperatures (1-3), and, given its high modulus and low density, is a promising candidate for weight-limited cryogenic structures. Some of these structures must be welded; hence the cryogenic mechanical properties of 2090 weldments are also important.

There have been numerous studies of the mechanical properties of Al-Li weldments at 293 K (4-8). In these studies, the base metal temper is ordinarily in the peak-aged condition and the fusion zone is in as-welded condition. Since the fusion zone does not experience the thermal-mechanical processing of the base metal, there is a strength mismatch in the weldment. As a result, inhomogeneous deformation and failure occur in the fusion zone. Recent work investigated the effects of processing on the tensile properties of 2090 weldments (9). Even with post-weld aging there is a continuing problem of strength mismatch and an inverse relation between the weldment strengths and elongation. An ideal process would be to post-weld solution heat treat and age the weldments, but it will be difficult to accomplish in real application due to size limitations.

The design of welded structures for cryogenic use requires a knowledge of the properties at temperature. The present work investigated the influence of base metal temper and filler metal additions on the tensile properties of 2090 weldments at 293 K and at 77 K. The influence of the base metal temper was studied to determine the effect of strength mismatch on the weldment properties. The use of Cu and Mg as solid solution strengtheners on the weldment was also examined.

Experimental Procedure

The chemical composition of 2090 is, in wt-%, 3.0 Cu-2.2 Li-0.12 Zr-Al. The as-received base metal sheet temper is in the T3 condition (solution heat treated and stretched 4.6%). The dimensions of the weld coupons were 102 mm x 152 mm. Some weld coupons were aged at 160°C for 16 hours to a near peak-aged condition, T8, and were subsequently machined down from 4.3 mm to 3.2 mm to remove the processing oxide and eliminate distortion. Prior to welding, the weld coupons, and filler additions, were degreased and chemically cleaned sequentially with ethanol, 5 vol-% of sodium hydroxide in water, and concentrated nitric acid.

The chemical compositions of the filler metal additions used are, in wt-%, 6 Cu-Al, 3 Cu-4 Mg-Al, 6 Cu-4 Mg-Al, and 4 Mg-0.5 Sc-Al. Sc is added as a grain refiner. A square groove of 3.2 mm was machined in the center of the weld coupon, and a filler metal of dimensions 3.0 mm x 2.0 mm was fitted inside the groove. Approximately 40% dilution was obtained. For both autogenous and filler metal additions, gas tungsten arc (GTA) welding process was used with direct current straight polarity on base material in the T8 condition. The heat input for autogenous and filler metal additions were 330 J/mm and 635 J/mm, respectively. Different parameters were used for the filler additions to eliminate a problem with fusion boundary cracking caused by severe porosity. The travel speed was decreased from 6.4 mm/s to 2.5 mm/s and the current was adjusted accordingly. In addition, flow rate of shielding gas, 75% He and 25% Ar, increased from 12 L/min to 19 L/min. In both cases, the welds were produced transverse to the rolling direction in an inert atmosphere on a water-cooled chilled block. After welding the reinforcements were machined and the final thickness of the weldments reduced to 2.54 mm. The weldments were tested in tension in the as-welded condition at 293 K and 77 K. A 25.4 mm composite gage length consisting of both fusion zone and base metal was used for the tensile specimens.

Results

Influence of Base Metal Temper

The mechanical properties of autogenous weldments with different base metal tempers are presented in Table 1. As expected, in the T3 temper the base metal strengths were low and elongations were high. With subsequent aging the yield strengths increased by 75 % from 281 MPa to 496 MPa, but premature failure occurred at the clip pin, resulting in 1.0% elongation at failure. At 77 K, both the T3 and the T8 base metal strengths increased, with the T3 base metal showing a greater percentage increase in strength. The T3 base metal retained excellent elongation, 11%, while the T8 base metal elongation increased to 6%.

At 293 K, the primary difference with different base metal tempers was in the yield strengths; the T3 base metal weldments had a higher yield strength, but the UTS and elongation were similar. At 77 K, both weldments failed prematurely in the fusion zones, but the T3 base metal weldment properties were better than that of the T8 base metal weldments.

Table 1 - Influence of base metal temper on the as-welded autogenous GTA weldment properties at 293 K and at 77 K.

	Base Metal Temper	Test Temp. K	YS MPa	UTS* MPa	Total Elongation %
Base Metal:	T3	293	281	352	11.2
	T8	293	496	523*	1.3
	T3	77	343	460	11.6
	T8	77	523	626	6.2
Weldment:	T3	293	178	267	3.5
	T8	293	144	264	3.3
	T3	77	237	333*	2.2
	T8	77	174	256*	1.5

* Fracture strength.

The deformation was concentrated in the fusion zone and necking occurred prior to failure. The notable difference between the T3 and T8 base metal weldments was that for the T3 base metal weldments, deformation extends into the heat affected zone (HAZ). For the T8 base metal weldments, there was necking at the center of the fusion zone, but there was no visible deformation extending into the HAZ. At 77 K, there was less deformation in the fusion zone for both tempers. The fractographs in Figure 1 show the T8 base metal weldments at 293 K and at 77 K. At both temperatures, the fracture mode was mixed with ductile dimples and secondary cracking along the dendrite boundaries. However, at 77 K fracture became predominantly interdendritic.

Influence of Filler Metal Additions

The mechanical properties of weldment with various filler metal additions are presented in Table 2. With 6 Cu addition, the mean Cu content increased from 3.0 wt-% to 3.7 wt-% and Li decreased from 2.2 wt-% to 1.6 wt-%. With Mg-Sc addition, Mg content increased to 1.4 wt-% while Cu and Li contents decreased to 1.4 wt-% and 1.4 wt-%, respectively. Except for the Cu addition, the changes in weldment properties were surprisingly small for the changes in the fusion zone composition. Vickers hardness traces across the fusion zones revealed that the autogenous and 6 Cu-added fusion zones were the softest with an averaged hardness number of 105, while the fusion zone of 6 Cu-4 Mg addition was the hardest with an averaged hardness number of 135.

With a Cu addition only, the room temperature yield strength of the weldments is low, but the elongation is superior to that of the Mg-containing additions by more than 300% and the UTS is roughly the same. In addition, the weldments with Cu-Mg additions tended to fail prematurely. The yield and ultimate strengths of the 6 Cu addition increased significantly on decreasing the temperature to 77 K while the elongation remained high.

The other filler additions had higher yield strengths, but failed prematurely. At both temperatures, the elongations of 6 Cu addition were significantly better than that of the base metal.

Table 2 - Influence of filler metal additions on the as-welded GTA weldment properties at 293 K and 77 K.

Filler Metal Addition	Test Temp. K	YS MPa	UTS* MPa	Total Elongation %
6 Cu-Al:	293	137	267	14.0
4 Mg-0.5 Sc-Al:	293	172	268	4.4
3 Cu-4 Mg-Al:	293	175	246*	1.3
6 Cu-4 Mg-Al:	293	181	259*	1.6
6 Cu-Al:	77	172	372*	10.3
4 Mg-0.5 Sc-AL:	77	225	-	0.2
3 Cu-4 Mg-Al:	77	-	217*	0.1
6 Cu-4 Mg-Al:	77	-	186*	0.1

* Fracture strength.

Even with filler metal additions, deformation is localized in the fusion zone. For the 6 Cu addition, the fusion zone necking occurred at both temperatures, and deformation extends into the HAZ at 77 K. With Mg+Sc addition, necking occurred in the fusion zone at 293 K, but at 77 K, there was very little plastic deformation. The Cu-Mg additions produced brittle weldments even at 273 K.

Figure 2 shows SEM micrographs of polished autogenous, 6 Cu, Mg-Sc, and 6 Cu-4 Mg added fusion zones. With increasing Cu content solute segregation is more pronounced. Mg additions led to a more cellular dendrite morphology. The fusion zone of the 6 Cu-4 Mg added weldment showed pronounced solute segregation between the cellular dendrites. These changes in the fusion zone microstructure influenced the fracture mode. Figure 3 shows fractographs of the 6 Cu and 6 Cu-4 Mg added weldments at 293 K. The fracture surfaces show distinctly different fracture modes. The 6 Cu added weldment failed in shear and the fracture surface appeared planar with slanted dimples. The fracture mode of Cu-Mg additions was similar, predominantly interdendritic; with 6 Cu-4 Mg addition, the dendrite surfaces of fractured weldment appeared brittle even at 293 K (Fig. 3b). The fractographs of Mg-Sc added weldments are shown in Figure 4. As the temperature decreased the fracture mode changed from mixed to predominantly interdendritic.

Discussion

Current practice in the industry is to peak-age the base metal prior to welding and to utilize the weldment in the as-welded condition. With the T3 base metal temper, the joint efficiency (the ration of the yield strength of weldment to that of the base metal.) is only 63%. As the strength of base metal increases, the strength mismatch increases and joint efficiency decreases to 29%. Deformation is confined to the fusion zone and the strain localization which develops results in premature weldment failure. A similar effect is seen at 77 K. It is, therefore, unnecessary to peak-age the base metal when the weldment is going to fail in the fusion zone. Even with filler metal additions to increase the weld strength, the strength mismatch continues to exist at both temperatures.

It is difficult to obtain a significant increase in weld strength by adding elements to the fusion zone without post-weld aging. On the other hand, the weld elongation is improved significantly by a Cu addition. Cu-added weldments have the best UTS and elongation combination at 77 K. Mg additions induce embrittlement at 77 K. All the Mg-added weldments failed prematurely at or prior to yielding. Ishchenko, et al.(10) examined the cryogenic weldment properties of Al-Mg-Mn alloys, and also reported brittle fracture at low temperature. However, they attributed the embrittlement to the Fe and Si contents.

Prior studies of Al-Cu-Li-Mg base metal alloys also show that the alloys tend to fail intergranularly. Several mechanisms have been proposed to interpret this behavior. Owen, et al.(11) have identified S phase (Al_2CuMg) and Fe-Cu rich intermetallic, Al_6(Fe,Cu), that tend to form at the grain boundary in the as-cast material. Even after solution heat treatment the Fe-rich phase remain present at the grain boundary. They concluded that the Fe-rich phase nucleates voids at the grain boundary, subsequently leading to premature cracking and reduced ductility. Miller, et al.(12), on the other hand, identified grain boundary precipitates of δ- and T-phases, or Fe-Cu rich intermetallic that may contribute to intergranular failure. Tramp elements, such as Na, K, and Ca, may also play a role. A different mechanism was proposed by Dew-Hughes, et al.(13) who suggested that intergranular failure intrudes at low temperature because the strength of the grain interiors increases more rapidly than that of the grain boundary.

The interdendritic fracture of Mg-containing weldments in the present work seems to be associated with intermetallic phases in the boundaries. As shown in Figure 2, with Mg additions microstructure becomes cellular dendritic with interdendritic phases outlining the boundary. The boundary phases have not been identified, but probably include the Mg-rich S phase (Al_2CuMg)(14) since they are much more pronounced when Mg is present. X-ray microanalysis (EDX) shows insignificant concentrations of Fe or Si in the fusion zones; hence, Fe-Cu rich intermetallics are unlikely to be the cause of embrittlement.

Conclusion

The base metal temper influences the cryogenic mechanical properties of autogenous weldments of 2090, especially at 77 K. At both room temperature and 77 K the T3 base metal has better weldment properties than the T8 base metal. In both cases, inhomogeneous deformation occurs in the fusion zone, but only the T3 base metal weldments have deformation extending into the heat affected zone.

The addition of Cu and Mg to the weld metal does not significantly increase the strength without post-weld aging. However, the Cu addition leads to a substantial increase in elongation. At 77 K, the 6 Cu addition leads to the best combination of UTS and elongation of the weldments tested. Mg additions cause embrittlement , particularly at 77 K, due to formation of a network of intermetallics at the dendritic boundaries..

Acknowledgement

The authors are grateful to Alcoa for research material. This research was supported by the Director, Office of Energy Research, Office of Basic Energy Science, Material Sciences Division of the U.S. Department of Energy under Contract No. DE-AC03-76SF00098.

References

(1) Glazer, J., Verzasconi, S.L., Dalder, E.N.C., Yu, W., Emigh, R.A., Ritchie, R.O., Morris, J.W., Adv. Cryo. Eng., Vol. 32, 1986, pp. 397-404.

(2) Glazer, J., Verzasconi, S.L., Sawtell, R.R., and Morris, J.W., Metall. Trans., 18A, pp. 1695-1701.

(3) Staley, J.T., Rioja, R.J., Wyss, R.K., and Liu, J., Alcoa Laboratory Technical Center Division Report 04-87-KD-34-56 , 1987.

(4) Pickens, J.R., Langan, T.J., and Barta, E., Aluminium-Lithium Alloys III, Proc.Conf. eds. C. Baker, P.J. Gregson, S.J. Harris, and C.J. Peel, The Institute of Metals, 1985, pp. 137-147.

(5) Le Poac, P., Nomine, A.M., and Miannay, D., J. de Physique, Vol. 48, No. 9, 1987, pp. 301-306

(6) Bowden, D.M. and Meschter, P.J., Scripta Metal, Vol. 18 , 1984, pp. 963-968.

(7) Edwards, M.R. and Stoneham, V.E., J. de Physique, Vol. 48, No. 9, 1987, pp. 293-299.

(8) Martukanitz, R.P., Natalie, C.A., and Knoefel, J.O., Alcoa Laboratory, PREN Division Report 52-87-20, 1987

(9) Sunwoo, A.J. and Morris, Jr., J.W., to be published in American Welding Society Journal.

(10) Ishchenko, A. Ya, Vasil'ev, A.D., and Stasyuk, S.Z., Adv. Cryo. Eng., Vol. 26, 1982, pp. 219-226.

(11) Owen, N.J., Field, D.J., and Butler, E.P., Mat. Sci. Tech., Vol. 2, 1986, pp. 1217-1222.

(12) Miller, W.S., Thomas, M.P., Lloyd, D.J., and Creber, D., Mat. Sci. Tech., Vol. 2, 1986, pp. 1210-1216.

(13) Dew-Hughes, D., Creed, E., and Miller, W.S., Mat. Sci. Tech., Vol. 4, 1988, pp. 106-112.

(14) ASM Metals Handbook, Vol. 8, 1973, p. 386.

Lists of Figures

Figure 1: SEM fractographs of as-welded autogenous 2090 weldments tested at a) 293 K and b) 77 K.

Figure 2: SEM micrographs of polished a) autogenous b) 6Cu added c) 4Mg+0.5Sc added and d) 6Cu+4Mg added 2090 fusion zones.

Figure 3: SEM fractographs of a) 6Cu added and b) 6Cu+4Mg added 2090 weldments tested at 293 K.

Figure 4: SEM fractographs of 4Mg+0.5Sc added 2090 weldments tested at a) 293 K and b) 77K.

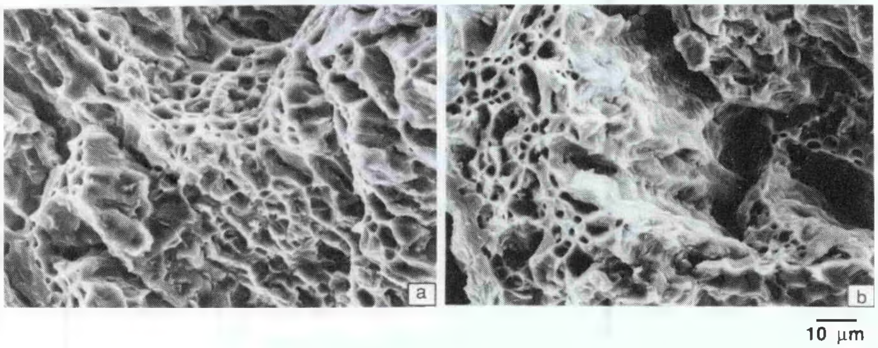

Figure 1

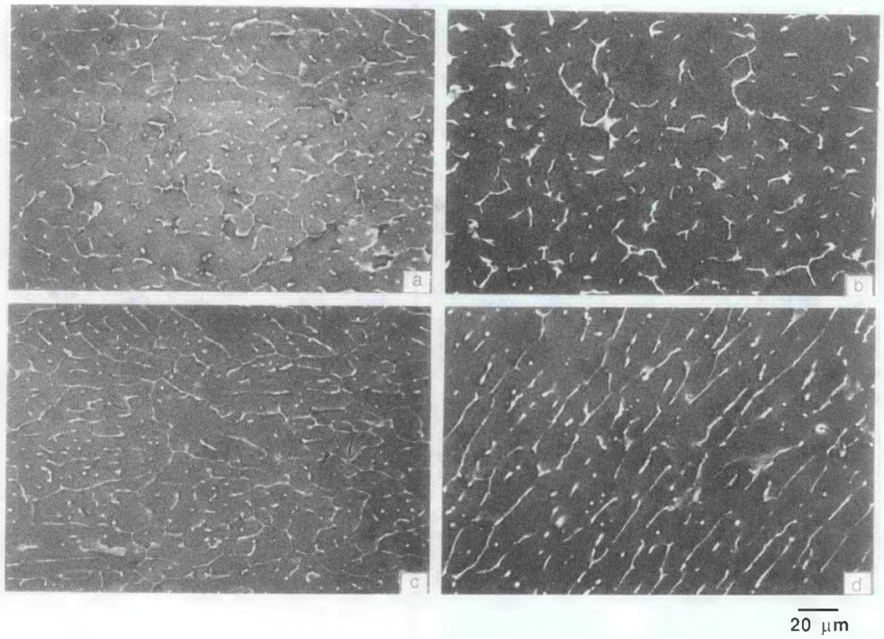

Figure 2

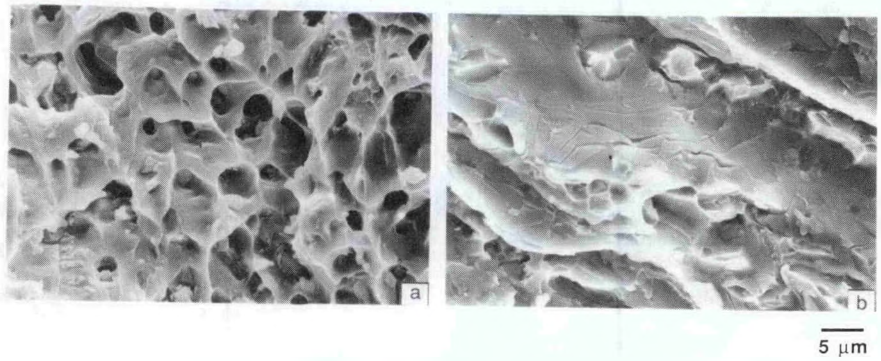

Figure 3

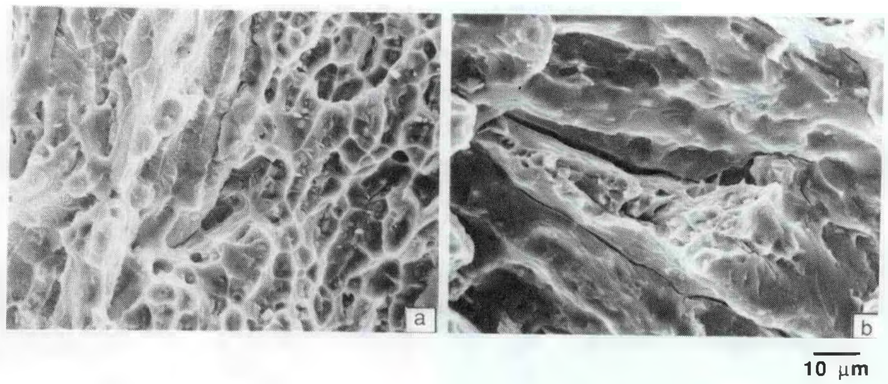

Figure 4